AFRL-AFOSR-VA-TR-2023-0451

Nanocomposites Through Cold Sintering: Designing the Intergranular Boundaries of Ceramics.

CLIVE Randall
PENNSYLVANIA STATE UNIVERSITY
201 OLD MAIN
UNIVERSITY PARK, PA,
US

09/15/2023
Final Technical Report

Air Force Research Laboratory
Air Force Office of Scientific Research
Arlington, Virginia 22203
Air Force Materiel Command

REPORT DOCUMENTATION PAGE

PLEASE DO NOT RETURN YOUR FORM TO THE ABOVE ORGANIZATION.

1. REPORT DATE	2. REPORT TYPE	3. DATES COVERED	
20230915	Final	START DATE 20190801	END DATE 20230531

4. TITLE AND SUBTITLE
Nanocomposites Through Cold Sintering: Designing the Intergranular Boundaries of Ceramics.

5a. CONTRACT NUMBER	5b. GRANT NUMBER	5c. PROGRAM ELEMENT NUMBER
	FA9550-19-1-0372	61102F
5d. PROJECT NUMBER	**5e. TASK NUMBER**	**5f. WORK UNIT NUMBER**

6. AUTHOR(S)
CLIVE Randall

7. PERFORMING ORGANIZATION NAME(S) AND ADDRESS(ES)
PENNSYLVANIA STATE UNIVERSITY
201 OLD MAIN
UNIVERSITY PARK, PA
US

8. PERFORMING ORGANIZATION REPORT NUMBER

9. SPONSORING/MONITORING AGENCY NAME(S) AND ADDRESS(ES)	10. SPONSOR/MONITOR'S ACRONYM(S)	11. SPONSOR/MONITOR'S REPORT NUMBER(S)
Air Force Office of Scientific Research 875 N. Randolph St. Room 3112 Arlington, VA 22203	AFRL/AFOSR RTB1	AFRL-AFOSR-VA-TR-2023-0451

12. DISTRIBUTION/AVAILABILITY STATEMENT
A Distribution Unlimited: PB Public Release

13. SUPPLEMENTARY NOTES

14. ABSTRACT
Cold Sintering offers a new processing method that permits the sintering of powders into dense strong materials at extremely low temperatures. The process involves a chemo?mechanical driving force that enables dissolution, transport, and precipitation to enable the densification of the powders. Typically, in powdered ceramics and metal materials this requires high temperature to densify the materials and as an approximate guide this is 50 to 80% of the melting temperature of the given materials. With cold sintering this can be as low as 10% of the melting temperature and thereby has an immediate attraction as a new strategy in sustainable production of materials. However, the focus of this study was to build upon the advantages of processing at such low temperatures. In particular, the study was concerned with exploring a broad suite of materials that can be cold sintered and developed into new materials and develop new
To help protect your privacy,
Micro so ft Office prevented
automatic downlo ad o f this
picture from the Internet.
AFOSR word mark
2
types of composites. To enable the formation of these materials we considered a combined fundamental approach to better understand the cold sintering process, along with engineering test cases on developing new materials. In the program we explored different chemical pathways to cold sinter and classified the different strategies. We developed a sintering model in that describes the early stages of the densification process. An important demonstration of introducing polymers into the grain boundaries of high permittivity materials to design the local field distribution that would benefit dielectrics in high? voltage energy storage applications. Demonstrations are given for improved resistivity, limiting nonlinear conduction at high fields, improving breakdown strength, suppressing voltage suppression of the relative permittivity at high fields in a ferroelectric material, and enhanced resistance to time dependent degradation processes. In electroactive materials for energy?storage we also demonstrated that cold sintering can potentially enable all solid?state batteries with the co?sintering of cathode and electrolyte materials. Also, in enhancing the volumetric energy densities and performance of cathode materials with the integration of nanolayers of carbon into the grain boundaries of cathode materials. This enables a cold sintering composite approach in designing the mixed ionic and electronic conduction control of the cathodes with optimized distributions of the phases. Finally, we considered the application of cold sintering to powdered metals to laydown the potential for complex metal ceramic composites, including new soft magnetic composites. Earlier we had shown that electrodes in multilayers can be densified but, in this case, we wanted to explore the densification of metals with larger particle sizes and note the potential new types of composites. We noted that under the compaction there is a coexistence of a plastic deformation and a cold sintering enhancement to the densification. We noted that the dihedral angles in the compaction process are redistributed with the cold sintering method relative to the normal warm compaction process. This also enhanced the mechanical strength, was consistent with the changes of the cohesion energy of the material, as determined through the contiguity model.

15. SUBJECT TERMS

16. SECURITY CLASSIFICATION OF:			**17. LIMITATION OF ABSTRACT**	**18. NUMBER OF PAGES**
a. REPORT	**b. ABSTRACT**	**c. THIS PAGE**		
U	U	U	UU	31

19a. NAME OF RESPONSIBLE PERSON	**19b. PHONE NUMBER** *(Include area code)*
ALI SAYIR	426-7236

Standard Form 298 (Rev.5/2020)
Prescribed by ANSI Std. Z39.18

Airforce Final Report:

Section 1: Structured Survey Questions

Award Information

- Award Number (Federal Award Identification Number **(FA9550-19-1-0372)**)
- Report Type: Final
- Principal Investigator: Clive Randall
- Principal Investigator Email: car4@psu.edu
- Principal Investigator Phone: (814) 863-1683
- Project Title: "Nanocomposites Through Cold Sintering: Designing the Intergranular Boundaries with Ceramics"
- Recipient Organization: The Pennsylvania State University
- Business Office Email: Nicole Wolfe, neh11@psu.edu
- Report Due Date: 31 August 2023
- Report Period Start: 1 August 2019
- Report Period End Date: 30 June 2023 (after 1 year no cost extension)
- Current Program Officer: Dr. Ali Sayer

Publications

1. Z.A.Grady, K.Tsuji, A. Ndayishimiye, J. Hwan-Seo, and C.A.Randall, ACS Applied Energy Materials 3 (5), 4356-4366, (2020), https://doi.org/10.1021/acsaem.0c00047

2. Z.A. Grady, J-H. Seo, K. Tsuji, A. Ndayishimiye, S. Lowum, S. Dursun, J-P. Maria, and C. A. Randall, "Cold Sintering for High-Temperature Electrochemical Applications", The Electrochemical Society Interface 29 [4] (2020) 59-65. https://doi.org/10.1149/2.F08204IF

3.A. Ndayishimiye, M.Y. Sengul, D. Akbarian, Z. Fan, K.Tsuji, S-H. Bang, A. C.T. van Duin, C.A. Randall, "Dynamics of the Chemically Driven Densification of Barium Titanate Using Molten Hydroxides", Nano Letters 21 [8] (2021) 3451–3457. https://doi.org/10.1021/acs.nanolett.1c00069

4.T. Sada, A. Ndayishimiye, Z. Fan, Y. Fujioka, C. A. Randall, "Surface modification of $BaTiO_3$ with catechol surfactant and effects on cold sintering", Journal of Applied Physics 129 (2021) 184102 https://doi.org/10.1063/5.0049905

5.T. Sada, Z. Fan, A. Ndayishimiye, K. Tsuji, S-H. Bang, Y. Fujioka, C. A. Randall, "In situ doping of $BaTiO_3$ and visualization of pressure solution in flux-assisted cold sintering", Journal of the American Ceramic Society 104 [1] (2021) 96-104. https://doi.org/10.1111/jace.17461

6.T. Sada, K. Tsuji, A. Ndayishimiye, Z. Fan, Y. Fujioka, C. A. Randall, "High permittivity $BaTiO_3$ and $BaTiO_3$ -polymer nanocomposites enabled by cold sintering with a new transient chemistry: $Ba(OH)_2{\cdot}8H_2O$", Journal of the European Ceramic Society 41 [1] (2021) 409-417. https://doi.org/10.1016/j.jeurceramsoc.2020.07.070

7.T. Sada, K. Tsuji, A. Ndayishimiye, Z. Fan, Y. Fujioka, C. A. Randall, "Enhanced high permittivity $BaTiO_3$–polymer nanocomposites from the cold sintering process", Journal of Applied Physics 128 (2020) 084103. https://doi.org/10.1016/j.jeurceramsoc.2020.07.070

8. Z Grady, Z Fan, A Ndayishimiye, CA Randall, "Design and sintering of all-solid-state composite cathodes with tunable mixed conduction properties via the cold sintering process." ACS Applied Materials & Interfaces 13 (40), 48071-48087, (2021). https://doi.org/10.1021/acsami.1c13913

9. T. Sada, K. Tsuji, A. Ndayishimiye, Z. Fan, Y. Fujioka, C. A. Randall, "Highly Reliable $BaTiO_3$ -Polyphenylene Oxide Nanocomposite Dielectrics via Cold Sintering", Advanced Materials Interfaces, 8 (18), 2100963, (2021). https://doi.org/10.1002/admi.202100963

10. L Paradis, D Waryoba, R Kyle, A Ndayishimiye, Z Fan, R Rajagopalan, C.A.Randall, "Densification and Strengthening of Ferrous Based Powder Compacts Through Cold Sintering Aided Warm Compaction" Advanced Engineering Materials 2200714, 1-11, (2022) https://doi.org/10.1002/adem.202200714

11. L Villatte, MI Rua-Taborda, A Ndayishimiye, CA Randall, A Largeteau, Graziella Goglio, Catherine Elissalde, Sylvie Bordère, Materialia 22, 101418, (2022) https://doi.org/10.1016/j.mtla.2022.101418

12. Ndayishimiye,A., Fan,Z., Mena-Garcia, J., Anderson, J.M., Randall, C.A., " Coalescence in cold sintering: A study on sodium molybdate", Open Ceramics,11,100293, (**2022**). https://doi.org/10.1016/j.oceram.2022.100293

Book Chapter:

Graziella Goglio, Arnaud Ndayishimiye, Catherine Elissalde, Clive Randall. Cold sintering and hydrothermal sintering. Michael Pomeroy. *Encyclopedia of Materials: Technical Ceramics and Glasses*, 1, Elsevier, pp.311-326, 2021, 978-0-12-822233-1. ⟨10.1016/B978-0-12-803581-8.12113-7⟩. ⟨hal-03311173⟩

Dissertations:

Zane Grady, Ph.D Dissertation, "Cold Sintering of Solid State Sodium Ion Battery Components," The Pennsylvania State University, **(May 2023)** https://etda.libraries.psu.edu/catalog/22992zmg19

Our servers will be contacting the Cross Reference open-source database (https://www.crossref.org/) to find any publications related to your award number. These

publications will automatically populate to your report page, and you will be able to select the reports that you would like to submit for the reporting period. Note: for annual/interim reports, you should only report publications that were completed in the current reporting period. For final reports, you should report all publications throughout the entire lifecycle of the grant.

If a publication does not show up in the initial publication search, you will also be able to manually enter publications using the publication's DOI number. Our servers will then contact Cross Reference to see if they can verify your publication information. Lastly, if your publication does not contain a DOI number, you can simply enter the bibliographic information into the text field.

Participants

Clive Randall Principal Investigator (48 months including no cost extension)
A. Ndayishimiye Post Doctoral Researcher (36 months) Worked on all Areas of the Project (Left PSU 2023 – Works in a Battery Materials Company in Maryland)
Z. Grady Graduate Student 36 months Worked on Electrochemical Systems- Graduated in 2023- works at PNNL.
Z. Fan Post Doctoral Researcher (12 months) Worked on TEM Characterization-Works at Los Alamos National Labs)
L Paradis Graduate Student (9 months) Worked on Metals
T. Sada Visiting Scientist (24 months) Worked on $BaTiO_3$ and related dielectrics (Return to Japan 2022)
A. Vester (Undergraduate Research 24 months) Worked on ZnO Composites- Graduated with Joint BS and MS in 2023_ Works at GE Aerospace Division)
R. Rajagopalan Supervisor of L. Paradis and worked closely with members of this team.

Other Partners or Collaborators

C. Elissalde and Colleagues from CNRS Bordeaux -collaborated with theory of cold sintering. (This was all conducted by Zoom- no Foreign Travel) This was all in kind from their resources.

Accomplishments

- Impact: The papers associated with this program that are listed above are gaining significant interest in terms of reads and citations. The work is also being requested as Plenary and Invited Presentations at international conferences. There are national programs being developed in Europe, Japan, and China around this work. There are now special sessions emerging at international conferences on cold sintering.

- Changes, we extended a no-cost extension as we had some work delayed during the Covid period.

-Technical updates include completion of Zane Grady thesis and completing papers.

Section 2:

"Nanocomposites Through Cold Sintering: Designing the Intergranular Boundaries with Ceramics"

Abstract:

Cold Sintering offers a new processing method that permits the sintering of powders into dense strong materials at extremely low temperatures. The process involves a chemo-mechanical driving force that enables dissolution, transport, and precipitation to enable the densification of the powders. Typically, in powdered ceramics and metal materials this requires high temperature to densify the materials and as an approximate guide this is 50 to 80% of the melting temperature of the given materials. With cold sintering this can be as low as 10% of the melting temperature and thereby has an immediate attraction as a new strategy in sustainable production of materials. However, the focus of this study was to build upon the advantages of processing at such low temperatures. In particular, the study was concerned with exploring a broad suite of materials that can be cold sintered and developed into new materials and develop new types of composites. To enable the formation of these materials we considered a combined fundamental approach to better understand the cold sintering process, along with engineering test cases on

developing new materials. In the program we explored different chemical pathways to cold sinter and classified the different strategies. We developed a sintering model in that describes the early stages of the densification process. An important demonstration of introducing polymers into the grain boundaries of high permittivity materials to design the local field distribution that would benefit dielectrics in high-voltage energy storage applications. Demonstrations are given for improved resistivity, limiting nonlinear conduction at high fields, improving breakdown strength, suppressing voltage suppression of the relative permittivity at high fields in a ferroelectric material, and enhanced resistance to time dependent degradation processes. In electroactive materials for energy-storage we also demonstrated that cold sintering can potentially enable all solid-state batteries with the co-sintering of cathode and electrolyte materials. Also, in enhancing the volumetric energy densities and performance of cathode materials with the integration of nanolayers of carbon into the grain boundaries of cathode materials. This enables a cold sintering composite approach in designing the mixed ionic and electronic conduction control of the cathodes with optimized distributions of the phases.

Finally, we considered the application of cold sintering to powdered metals to laydown the potential for complex metal ceramic composites, including new soft magnetic composites. Earlier we had shown that electrodes in multilayers can be densified but, in this case, we wanted to explore the densification of metals with larger particle sizes and note the potential new types of composites. We noted that under the compaction there is a coexistence of a plastic deformation and a cold sintering enhancement to the densification. We noted that the dihedral angles in the compaction process are redistributed with the cold sintering method relative to the normal warm compaction process. This also enhanced the mechanical strength, was consistent with the changes of the cohesion energy of the material, as determined through the contiguity model.

Goals:

The overall goals of the AFOSR **(FA9550-19-1-0372)** program:

1). Better understanding of the cold sintering process, atomic mechanisms, and its general applicability.

2). Design new composites with better interfacial design.

3). Analysis and modelling the interfacial behavior with cold sintering.

1.0 Introduction

Conventional sintering occurs at high temperatures, typically ranging from several hundred to tens of hundreds of degrees Celsius, to enable mass transport processes and diffusion across the boundaries of adjoining particulates for atoms, cations, or molecular groups. For many materials such as a typical oxide, the sintering temperature is typically around 1000 ^{o}C and above, and the time to sinter even a simple pellet of dense material in the laboratory can be up to 2 to 10 hours. The sintering of solid inorganic particulates into a dense polycrystalline ensemble with a combination of thermal energy and pressure underpins the manufacturing production process for multitudes of different ceramic and powder metal products. Large-scale batch and continuous furnace technologies enable mass production but formed structures must undergo a long-time process where they are heated through various temperature-time profiles to control the density, microstructure, and associated properties of the resulting component.

Cold sintering was studied by the Randall group for a couple of years prior to the filing of a patent in 2015[1]. From this patent there are now several international/regional patents, including Europe, China, Canada, Japan, India (8), with 14 international companies licensing the core cold sintering technology from Penn State. Since then, there have been several papers demonstrating its applicability across different material systems by Penn State and others[1-12]. These have both confirmed initial findings and moved the field forward with new material examples that can be cold sintered, as well as introduced new scientific theories to address the enhanced diffusional process that permits such low-temperature sintering. The cold sintering process, with densification occurring in the range of 5 to 60 minutes, is enabled through diffusion in a transient liquid phase and uniaxial pressure, which originally took place in a simple laboratory polymer laminator press. Underpinning this phenomenon is a small quantity of a transient chemical phase (ca. 1 to 5 vol%) that needs to drive local dissolution from the surfaces and precipitation on the powder surface at the pores. These processes are enhanced with coupled effects of the applied pressure and temperature that drive the kinetics and enable high densities in short times. Cold sintering is impossible without the correct chemistry being matched to the used transient phase. The process can be enhanced with particle size, temperature, and solvent choice, or with other thermodynamic driving forces. **Figure 1** schematically demonstrates the basic sequence of mechanisms that enables the cold sintering process. The scientific details of these mechanisms are still being considered, but with over 200 materials being cold sintered, and multiple groups

around the world building from our work, there is no doubt that cold sintering offers a new breakthrough in material science. Within these materials they include a wide suite of critical applications such as electronic devices from varistors, dielectrics, sensors, battery, piezoelectric materials, as well as catalysis support materials such as zeolites, biomaterials, and structural applications. In the form of composites and able to process at low temperatures, we can in a bulk process and thick film multilayers all classes of materials namely ceramics, metals, and polymers. Given all these recent discoveries there are still so many areas to explore, and we believe the subject is still in its infancy. This AFOSR *(FA9550-19-1-0372)* program considered the basic concepts on how cold sintering mechanisms impact interfaces, design of properties in forming new types of nanocomposites.

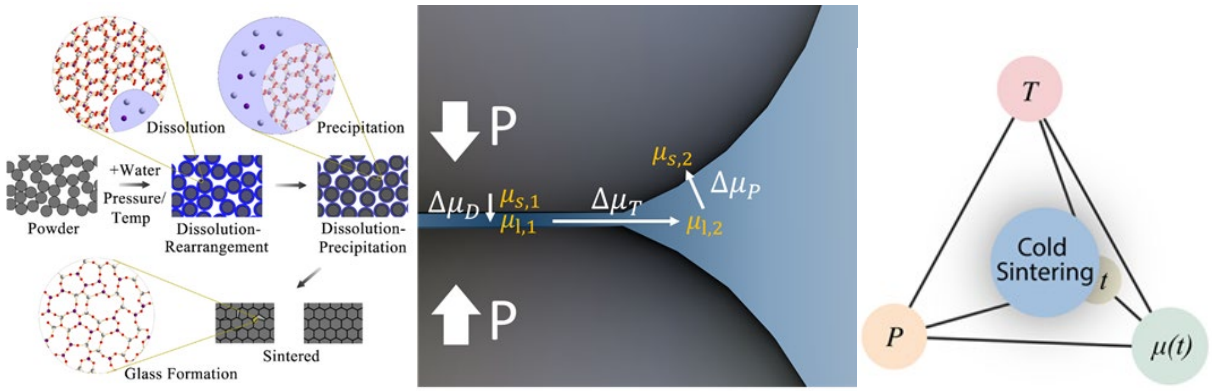

Figure 1*: Schematic showing the dissolution and precipitation processes that can be activated with the transient phase, moderate uniaxial pressures, and temperatures to drive the cold sintering process.*

In summary, the discovery of cold sintering presents many major new technological opportunities and advancements worldwide:

- Large energy and cost saving for ceramic sintering.
- Integration of different inorganic materials to create unique material properties.
- Flexible composite design with integration of ceramic, metal, and polymers in a single step
- Processing of novel composites and laminated materials.
- Large number of groups now involved in cold sintering with national programs in Europe, China and Japan all confirming and building beyond our initial work.
- Over 200 ceramic materials have now been successfully cold sintering.

- Hybrid processes incorporating cold sintering with other non-equilibrium sintering methods, such as Spark Plasma Sintering (SPS) offers great promise.

The unique composites could over several advantages in materials design to many strategic DOD applications. Below we will summarize the insights that have been gained under this AFOSR *(FA9550-19-1-0372)* program. There have been several strategic studies under this program to build knowledge and understanding with the forementioned project goals.

2.0 Better Understanding of the Cold Sintering Process

Cold sintering is a chemo-mechanical process that drives dissolution, transport, and precipitation. The selection of the all-important chemistry in the form of the transient phase that enables the dissolution is critical to cold sintering. If this phase has slow kinetics in dissolution and or cannot allow the precipitation, then cold sintering cannot proceed. So, a classification of different chemical approaches to aid the science of chemical selection for various systems was suggested and demonstrated.

2.1 Chemical Routes

Under the cold sintering, we proposed that there are three major different pathways to obtain dense materials as shown in **Figure 2**. In the first pathway, a compound, A, leads to the densification of the same compound A. So (A → A) as from the initial powder all the way to the final material with same composition and crystallographic phase. As demonstrations of the cold sintering process within a pathway of A → A, in a single-step densification, are shown with the paraelectric dielectric $SrTiO_3$ (Figure 2 b-d) and with the ferrite ceramic, $SrFe_{12}O_{19}$ (Figure 2 e-h).

Alternatively, there is a pathway where a compound A leads to a compound B (A → B), where the final material has a different chemical composition or crystallographic phase than the initial powder.

Finally, there exists the possibility for A + B → C, which is a reactive route, where a mixture of compounds A and B can either lead to a chemical doping of a similar phase or a transformation to a new compound after CSP. This approach is inspired by different low-temperature reactive (a) synthesis techniques using small amounts of solvents such as the water-assisted solid-state reaction, [13-17] salt molten synthesis with their high reactivity[18] and (b) densification techniques such as the reactive hydrothermal densification.[19]

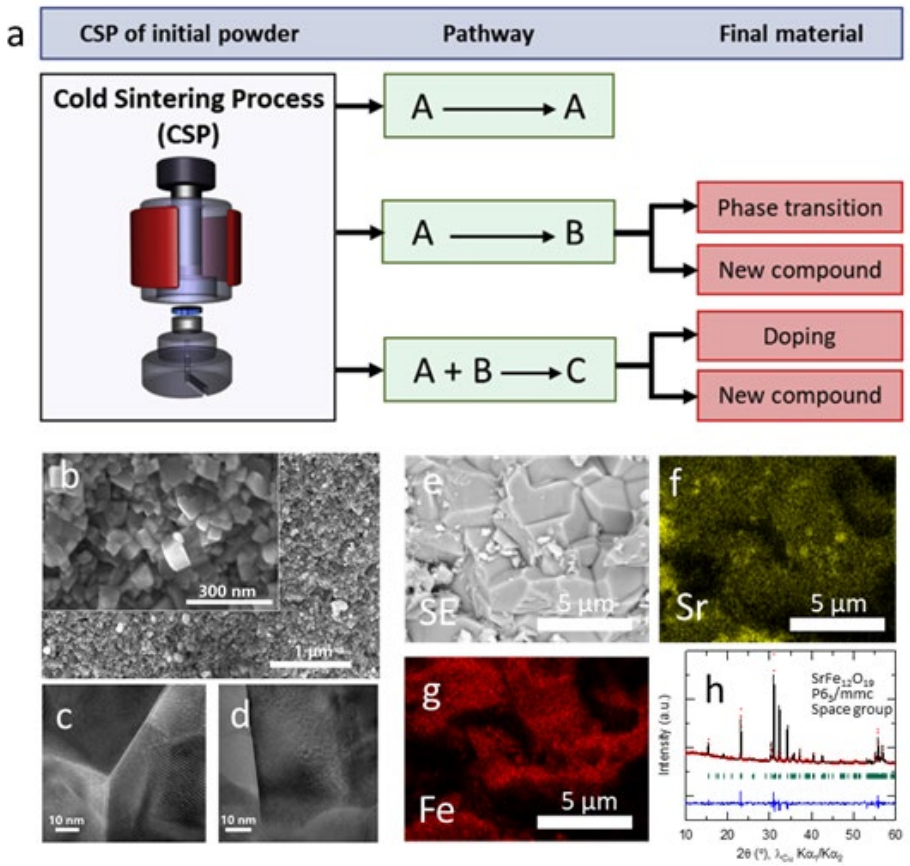

Figure 2 *: (a) Different chemistry pathways in cold sintering. Examples of compounds cold sintered using the A → A pathway; (b) SEM micrograph and (c,d) HR-TEM images of $SrTiO_3$ grain boundaries, cold sintered at 290 °C, 500 MPa using a NaOH flux and with a relative density of 97.7%. EDS analysis of a $SrFe_{12}O_{19}$ ceramic cold sintered with a $Sr(OH)_2.8H_2O$ flux at 250 °C, 350 MPa and with a relative density of 87.0 %: (e) secondary electron – SE – image and elemental maps of (f) strontium – Sr and (g) iron – Fe. (h) Rietveld refinement of the cold sintered $SrFe_{12}O_{19}$ ceramic to highlight a good phase purity.*[20]

3.0 Cold sintering mechanisms

Densification with CSP is mainly based on the pressure solution creep mechanism. This mechanism, often encountered in geosciences, is driven by chemical potential gradients from highly constrained areas with enhanced dissolution and high chemical potential to low constrained areas at particle surfaces with a lower chemical potential, through atomically thin liquid film at the contacting particle surfaces **Figure 1**. The understanding of events/phenomena occurring during and after pressure solution is critical to effectively select appropriate solvents enabling

densification and design scale up strategies. The pressure solution creep mechanism allowing low temperature atomic processes and is associated with the densification of geological sedimentary rock formations. **Figure 3** shows the various mechanisms that can enable deformation in a model crystal structure such as Halite. These include dislocation glide, high temperature bulk and grain boundaries creep processes, and at low temperatures in the presence of a transient chemical phase, the pressure solution creep.[21]

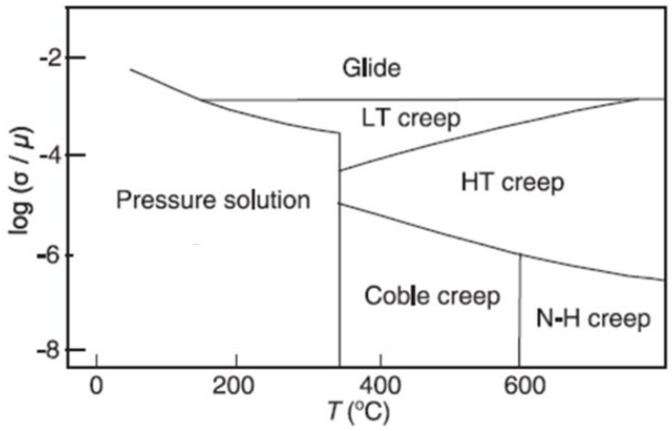

***Figure 3**: Deformation map of a model mineral, Halite over a range of applied stresses and temperatures[21].*

3.1 Understanding densification with molten hydroxide fluxes

To improve the fundamental knowledge of densification mechanisms with a chemical perspective in cold sintering using molten salts, experimental studies combined with reactive force field (ReaxFF) molecular dynamics simulations were conducted on the $BaTiO_3$/NaOH-KOH system. The detailed investigation has shown the importance of transient complexes formation in the dissolution process of both Ba and Ti ions.[22] The dissolution of Ti, which is the most challenging in $BaTiO_3$, takes place through unstable and soluble NaTiO complexes **Figure 4** (a). The extent of dissolution in the system is sufficient to efficiently drive densification of $BaTiO_3$ as a relative density of 90% is reached in less than about 50 min. With longer sintering times, translucency of cold sintered pellets can be obtained as more residual solvent and pores are eliminated from the material system **Figure 4** (b).

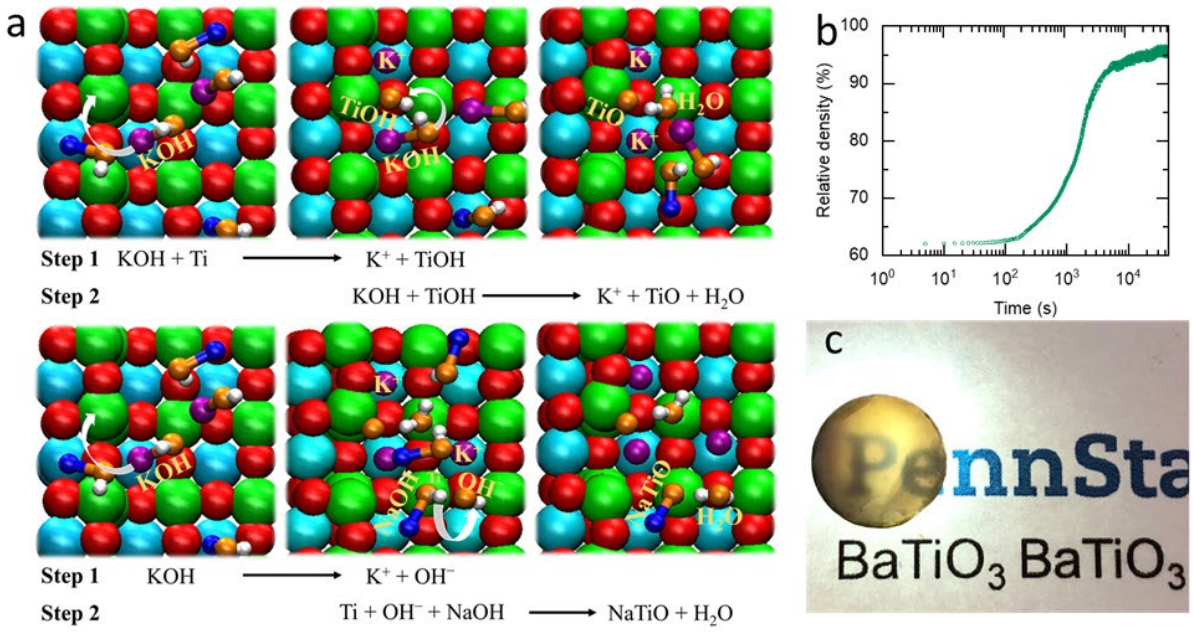

Figure 4 *: (a) Representation of the major chemical reactions observed at the interface with ReaxFF MD simulations. Key: barium (light blue); titanium (green); potassium (purple); sodium (blue); oxygen atoms in $BaTiO_3$ (red); oxygen atoms of hydroxides (orange); hydrogen atoms (white); (b) $BaTiO_3$ time-dependent evolution of the relative density; (c) photograph highlighting a $BaTiO_3$ translucent sample obtained by cold sintering.*[22]

3.2 Grain Growth: Ostwald Ripening and Coalescence

In sintering a material there is a general competition to the minimization of the excess surface energy through either grain coarsening or densification that removes high energy surface energy between grains and particles. This competition determines the microstructure and grain growth can limit the final densification. Relative to other sintering methods the densification of a powder compact is superior compared to grain growth under the cold sintering process. Earlier we have demonstrated that grain growth follows in for example a model system such as, ZnO, with a $G\text{-}G_o \sim Kt^{1/n}$ isothermal grain coarsening, with n=3, G_o is the initial grain size, K is a rate constant, and t, is time.[23] In cold sintering, phenomena such as nucleation, Ostwald ripening and coalescence can all take place during or after the precipitation stage of pressure solution creep. The growth can have both mechanisms operating, and the degree seems to be determined by the specific system and a transient chemistry. Below we summarize examples of these findings under the cold sintering process. Ostwald ripening can be deduced in the case of $BaTiO_3$ with the use of alkali fluxes, as described above. **Figure 5** shows the microstructure of a $BaTiO_3$ sintered with a) NaOH-KOH flux, and b) the flux $SrOH{:}8H_2O$. A core shell microstructure is shown in **figure 5** (a), using the small hydroxyl precipitates that

existed in the initial powder and under the cold sintering a shell region is noted that has eliminated these nano-precipitates. In the case of $SrOH{:}8H_2O$, we see evidence of a core shell microstructure with energy dispersive spectroscopy, the strontium cations are soluble in the shell. So, we inferred that small particles with the higher surface areas are undergoing dissolution and then reprecipitation has occurred under the processing.

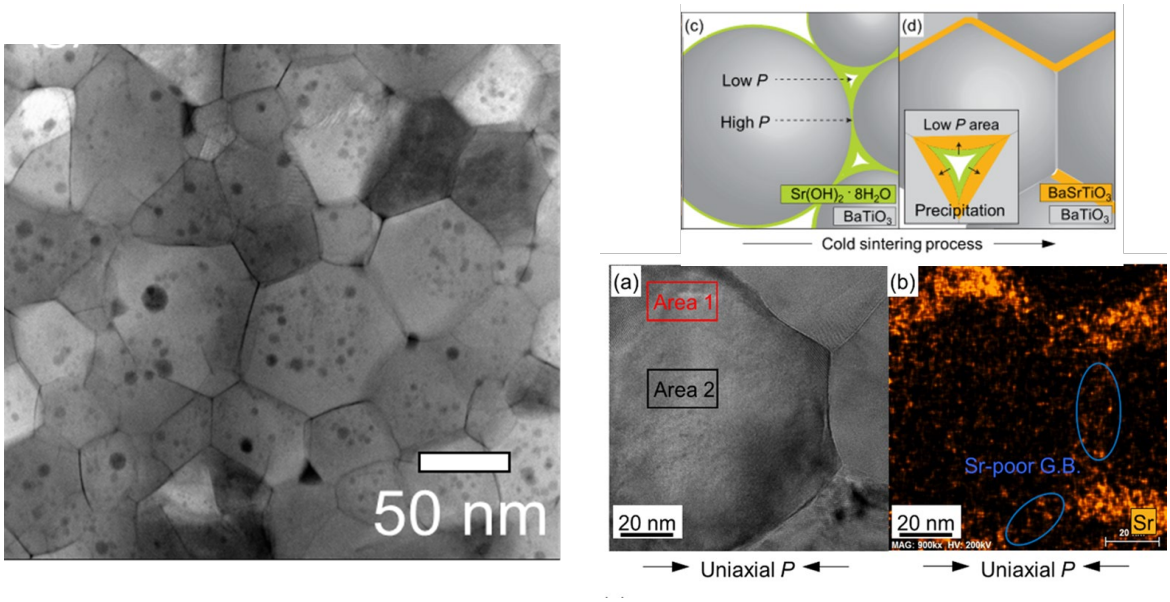

***Figure 5**: Core-shell evidence in the growth process of $BaTiO_3$ in the cold sintering process, a) shell region without hydroxyl precipitates, and b) the Sr- solubility from the $SrOH_2{:}8H_2O$ sintering flux.*[24,25]

As an alternative material we considered the chronology of the events and temporal evolution, of a $Na_2Mo_2O_7$ / H_2O system sintered at 200°C and 350 MPa. This system highlights fast transformations and densification during cold sintering **Figure 6** (b,c,d). Early observations confirm events such as long-range mass transport in this material system as $Na_2Mo_2O_7$ is highly soluble in H_2O (Areas highlighted in yellow - **Figure 6**(d). After longer sintering times, features that may be related to ongoing Ostwald ripening (Blue arrow – **Figure 6 (**b)), coalescence with the array of aligned pores (Areas highlighted in red – **Figure 6 (**c)), probably highlighting earlier location of a grain boundary in accordance with pressure solution studies by Zhang and Spiers.[26]Microstructural study of reconsolidated salt and sub grain boundaries (Area highlighted in green – **Figure 6** (c)), likely resulting from coalescence. Further detailed analysis of grains of this type can support the coalescence mechanism for this system, is shown in **Figure 7** with a scanning electron microscopy (SEM) and transmission electron microscopy study. In these images we capture crystallographic orientation between some of the grain with entrapped residual fluxes from the gel

formed after the dissolution of the sodium and molybdate constituents. That with the water forms NaOH, and Molybdic acid that undergoes a gelation with the water loss. For similarly orientated neighboring grains there is a coalescence, with a series of entrapped glassy phases along the interface. So $Na_2Mo_2O_7$ / H_2O shows evidence of both Ostwald ripening and coalescence grain growth under cold sintering.

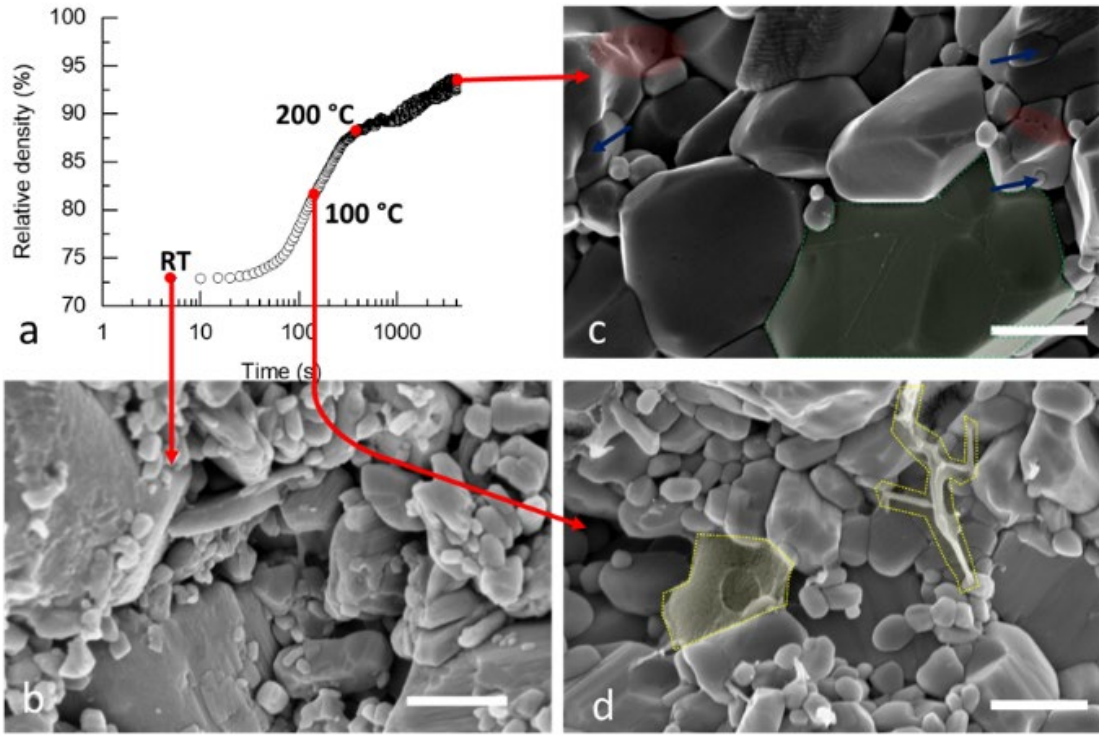

Figure 6: *(a) $Na_2Mo_2O_7$ time-dependent evolution of the relative density, SEM micrograph of a (b) green $Na_2Mo_2O_7/H_2O$ pressed pellet, (c) $Na_2Mo_2O_7$ ceramic cold sintered at 200 °C, 350 MPa for 60 min. The blue arrows are pointed to grains probably ongoing Ostwald rippening; the area in red highlights earlier location of grain boundaries; the area in green highlights a grain with subgrain boundaries; (d) $Na_2Mo_2O_7$ ceramic quenched at 100 °C. The area in yellow highlights long-range mass transport during cold sintering.*[27]

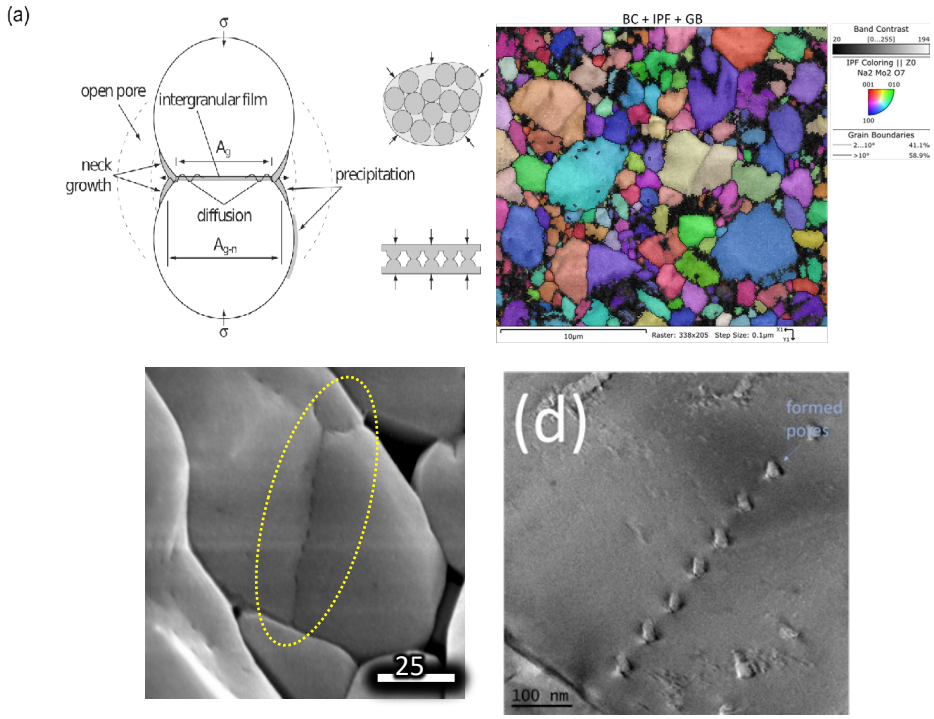

***Figure** 7: (a) Schematic of a rough interface that can lead to entrapped gels, (b) electron back scattering diffraction of grain structure with small angle tilt boundaries within larger grains of $Na_2Mo_2O_7$, (c) and (d) trapped pores at the boundaries.*[26,27]

4.0 Metal Cold Sintering

CSP helps to significantly improve the green strength and densification of powdered metal iron compacts. The powder preparation approach leads to the formation of ultrathin co-continuous phosphate layer at the iron particle interfaces, which contributes to the dissolution-precipitation creep densification mechanism in addition to plastic deformation **Figure 8** (a), which is predominant for metals. Using this powder processing approach leads to an increase of the compact's green strength by almost six times, making green machining **Figure 8** (b) such as threading and grooving of metal compacts possible **Figure 8** (c',c"). The conventional sintering of cold sintered compacts leads to dense materials **Figure 8** (d) improved mechanical strength **Figure 8** (e). The cold sintering of metals may offer major new opportunities in the powder metallurgy industry. Furthermore, this approach can also be applied to several other metal systems and will likely be of significant interest to the materials community.

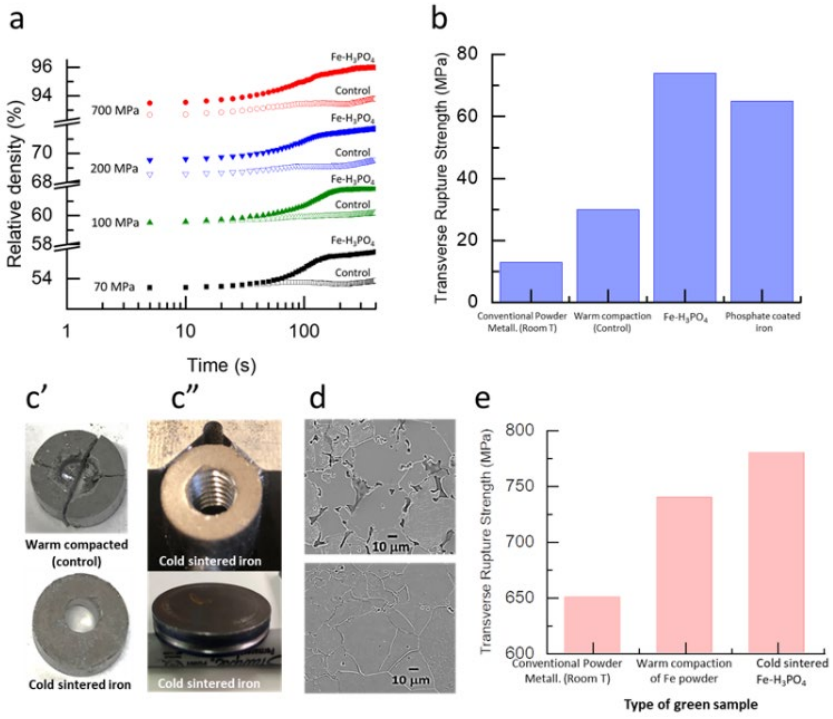

Figure 8 *: (a) Evolution of the relative density of plain iron (control) and iron coated with phosphoric acid (Fe-H_3PO_4) compacts as a function of time when subjected to different pressures (70, 100, 200 and 700 MPa), at a constant heating rate in the anisothermal region; (b) Comparison of transverse rupture strength of conventional PM iron compact, Warm compacted iron, Fe- H_3PO_4 compact and phosphate coated iron compact hot pressed at 620 MPa and 140 °C; Machinability of cold sintered warm compacted iron (control) (c', top) relative to Fe- H_3PO_4 (c', bottom) ; (c", top) threaded 0.5" diameter cold sintered Fe- H_3PO_4; (c", bottom) grooved 2" diameter cold sintered Fe- H_3PO_4; Scanning electron micrograph of etched conventional sintering at 1175 °C under 90% Nitrogen 10% Hydrogen atmosphere, from (d, top) warm compacted iron and (d, bottom) cold sintered Fe- H_3PO_4 green pellets. (e) Comparison of transverse rupture strength of conventionally sintered iron obtained from different types of green materials: room temperature conventional powder metallurgy process, warm compacted iron and cold sintered Fe-H_3PO_4.*[28]

The ability to sinter metals with a strategic coating of a transient chemistry is a powerful finding. In several ways, below we summarize the technological and the scientific advancements that can be built upon with this discovery. Let's start with the technological advantages, above, and in the published paper by Paradis et al, where detailed experimental information can be found.[28] We perform the demonstration in a commercial warm pressing die that is used in the powder metallurgy industry, with commercial powders. The mechanical strength of these cold sintered compactions is sufficiently improved above the typical commercial warm compaction conditions, and permits the ability to machine the components, as shown in Figure 8 (c', c"). This can reduce wear on milling/ machining that perform

cutting, grooving, and drilling, such as drills, threading tool pieces, as examples. The ability to sinter metals, also gives a unique opportunity to sinter complex mixtures of different metals and cermet composites.

Although, we do not fully understand the cold sintering of metals, we note that the increase in the compaction strength is also having a redistribution of the dihedral angles at the triple points. We applied the Randall-German theory of quantifying the dihedral angles via the Contiguity factor, C_{ss}, and scaling to the measured compact strengths.[29] The Contiguity factor is a quantification of the interphase contact and relates directly to the cohesive strength of the grain boundaries. There is a clear demarcation between the conventional compaction and the cold sintered assisted approach, as shown in **Figure 9**. With the Contiguity factor for cold sintered sample range between 0.55 and 0.76, well above the critical value 0.38.

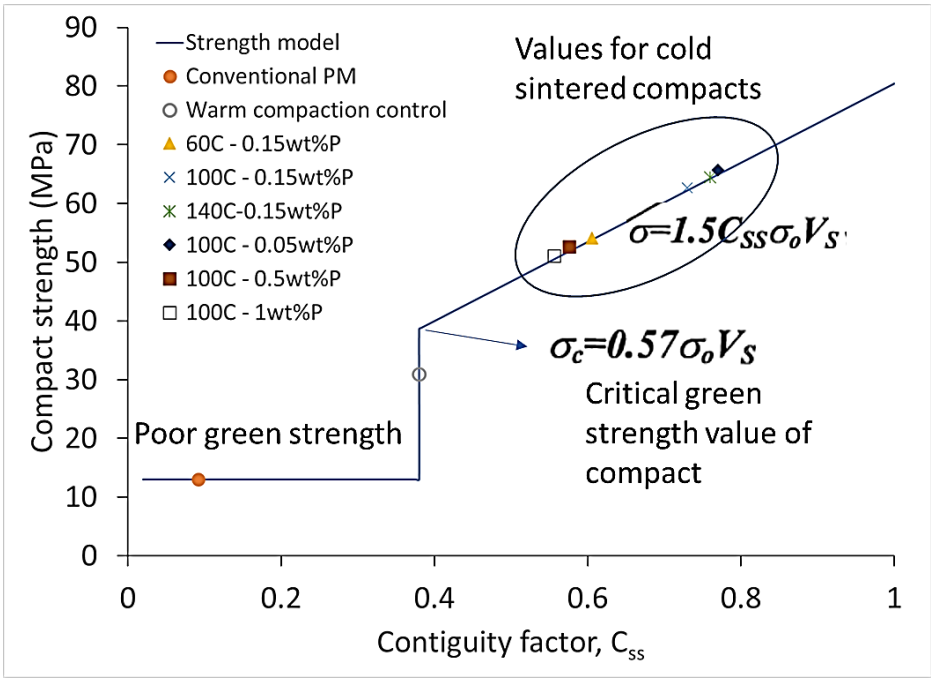

***Figure 9**: Compaction Strength versus Contiguity Factor for different compaction processes.*[28,29]

5.0 Designing New Composites with Cold Sintering

One of the important advances that is possible with cold sintering is enabled with the process temperatures and times, being low and fast, that limits the compatibility between the composite phases. Ideally when we are designing composites, we are

trying to mix different materials together and have predictable properties that are the result of the spatial interconnectivity, and the relative volume fractions of the respective phases, without a chemical interaction between these phases. So here we will investigate some different composites that all possess different challenges and opportunities under the cold sintering process.

5.1 $BaTiO_3$ Polymer Dielectric Composites

$BaTiO_3$ polymer composites have been considered before, and typically the volume fraction of the $BaTiO_3$ powders is ~ 40 to 60 volume percent, and the polymer with a low dielectric constant ~2 that with the serial mixing and high-volume fractions limits the overall magnitude of the composite permittivity to a relative permittivity to ~ 40 to 60, well below the permittivity of the ceramic $BaTiO_3$ that is ~2500. So, the difficulty in such composites has always been the ability to remove porosity, and to enhance the permittivity with higher volume fractions of $BaTiO_3$. Cold sintering potentially offers such a route if a transient chemical phase can be found that can be co-processed with the polymer, avoiding decomposition through either thermal or chemical deleterious reactions. Below we will demonstrate several major advantages in dielectric properties in fabricating a $BaTiO_3$ polymer composite with cold sintering. We consider these advantages coming from the high resistive and low permittivity polymer phases that change the electric field distribution across the dielectric, and therefore less local field control the overall properties. The local fields then in principle should reduce the field effects in the ferroelectric materials. **Figure 10** shows a schematic of the field distribution in these new types of dielectric materials.

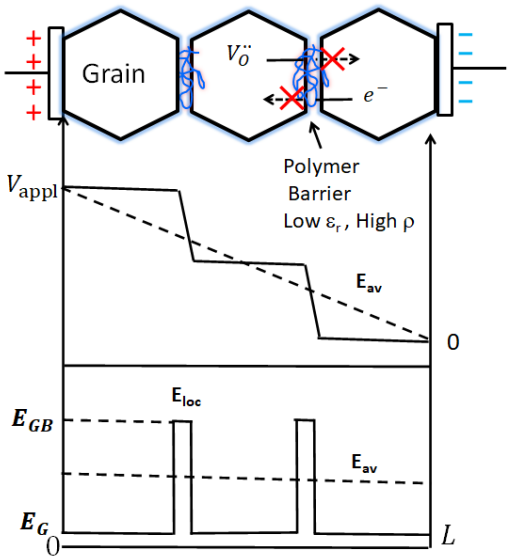

Figure 10: *The schematic demonstrates the partitioning of the field in a microstructure where the polymer and $BaTiO_3$ phases having vastly different permittivity, dilutes the field in the grains and enhances the field in the polymer, because of the continuity of the displacement field, $\underline{D}$.*

Here with cold sintering, we addressed the importance of improving the spatial distribution of a high temperature polymer in the grain boundaries of a $BaTiO_3$ dielectric.[30] The rationale of this design is to influence the local electric field distribution within the microstructure, to limit the conductivity, and degradation, and manipulate the temperature dependence of the dielectric permittivity. This is accomplished through a physical adsorption process, where an acetic acid surface treatment of powders permits interaction of a poly (p-phenylene oxide) (PPO) with the $BaTiO_3$ particle surfaces through hydrogen bonding.[31] This, then, undergoes a cold sintering process at temperatures ~225°C with the use of a $(BaOH_2)$:$8H_2O$ flux and a moderate uniaxial pressure, thereby produces a homogeneously dense dielectrics (>96% of theoretical) with different volume fractions of PPO. The basic process is illustrated in **Figure 11**. Whereas **Figure 12,** shows that a high-density microstructures with relative densities between 96% and 98%, and there is a small dependence of the final density with PPO content. This suggests that PPO does not hinder the interface reaction and the following densification regardless of the polymer amount.

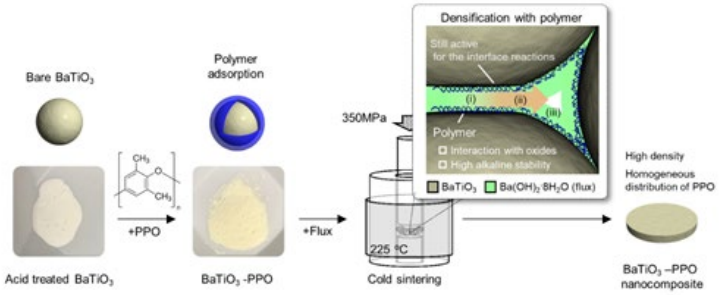

Figure 11: *Scheme for fabrication of $BaTiO_3$-PPO nanocomposites using cold sintering. PPO can adsorb on the surface of acid-treated $BaTiO_3$ through hydrogen bonding. The pressure-assisted interface reactions ((i) dissolution, (ii) diffusion, and (iii) precipitation of dissolved ions in the inset image) drives the densification even with adsorbed polymers at low temperature. Polymers have an appropriate interaction with oxides, which aids their homogenous distribution in the matrix without hindering the interface reactions.*[31]

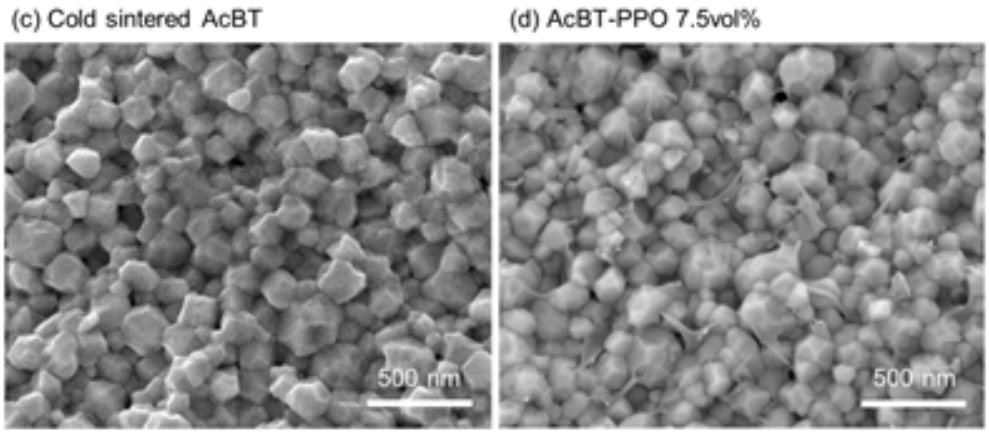

Figure 12*: **(a) and (b)** show SEM images of faceted microstructure of cold sintered AcBT with 0 and 7.5 vol% of PPO. Powders are transformed into dense microstructures with polygonal facets of oxides for both samples after cold sintering.* [31]

The temperature dependence of the relative permittivity and field dependence is influenced by the PPO content in a systematic manner. The superior resistivity by the homogeneous distribution of PPO varies in magnitude with volume fraction; it limits areas of field concentration and therefore also suppresses nonlinear conduction to higher fields. The magnitude of the permittivity follows a logarithmic mixing law that implies that there is an equal weighting of serial and parallel components with polymer addition, and this reflects a superior spatial distribution in the densified nanocomposite. We contrasted the $BaTiO_3$-PPO composite dielectrics under accelerated lifetime testing conditions noting superior resistance toward

degradation kinetics, indicating an important breakthrough opportunity towards the development of high reliability dielectrics.[31]

In **Figure 13,** we show that the polymer improves resistivity with the addition of the polymer PPO. The polymer also suppresses non-linear conductivity effects, and improves the breakdown, not shown here is also a major improvement in the reliability with a much longer time to undergo degradation due to oxygen vacancy migration. The polymer around each grain limiting any further migration of the oxygen vacancy, there is a confinement to the grains, with no long-range trans granular migration that typical leads to failure of dielectric materials under prolonged exposure to electric field and temperature. These conditions lead to the military rating of a capacitor, and so going forwards any process methodologies to improve these conditions is of major interest in DOD applications.

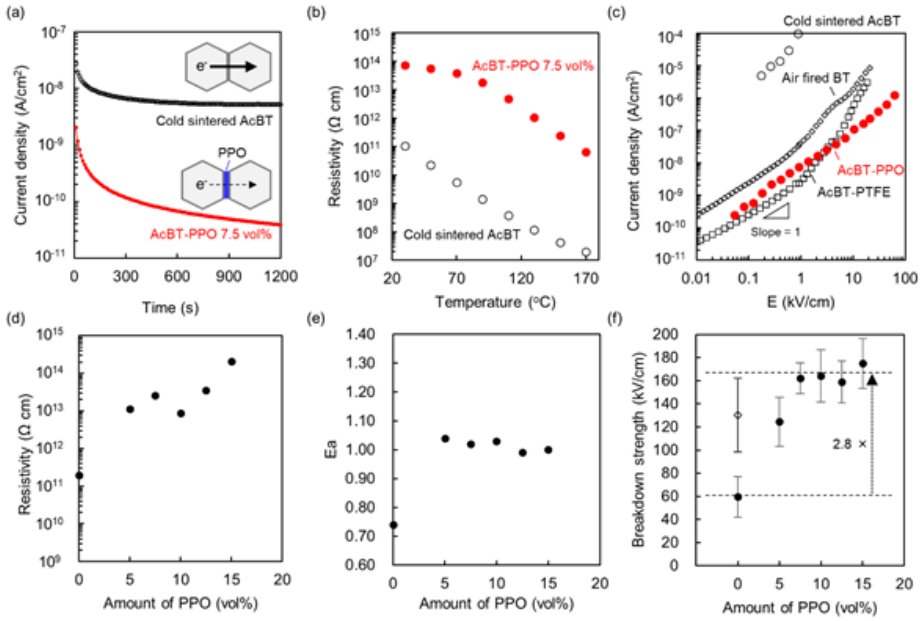

Figure 13: *(a) Changes in current density with time, (b) temperature dependence of the resistivity and (c) Current density - Electric field (I-V) characteristics at 150 °C for the cold sintered AcBT (black open circles) and the composite with 7.5 vol% of PPO (red solid circles). I-V characteristics for the composite with 5vol% of PTFE (open squares) and the conventionally air sintered $BaTiO_3$ ceramics (open diamonds) are also shown in (c). (d) Resistivity, (e) activation energy extracted in the natural logarithm Arrhenius plots using (d), and (f) the electrical breakdown strength (BDS) for the composites as a function of volume fraction of PPO. BDS for the conventionally air sintered BT ceramics of similar density and thickness (open diamonds) are also shown in (f).*[31]

This study in summary illustrated a $BaTiO_3$-PPO nanocomposite that was processed to improve the polymer distributions in the grain boundaries. This was enabled with

the interaction between PPO and an acid treated surface of $BaTiO_3$ powders. These powders are then cold sintered into extremely high-density dielectrics with the cold sintering process. The dielectric properties are controlled with a redistribution of local electric fields that suppress many of the deleterious mechanisms that limit high permittivity dielectrics. The key properties that have been determined include:

i. Composites with high relative permittivity ~ 1000 to 2000, and a dielectric loss tangent ~0.05
ii. Reduced temperature dependence of the permittivity with diffuse phase transitions, over a broad temperature window
iii. High resistivities, ρ, ~ 10^{13} to 10^{14} Ω cm at room temperature,
iv. Suppressed non-linear voltage saturation effects under high applied fields
v. Suppressed non-linear conductivity to high fields (~ 80 kV/cm) and high temperatures ~ 150 ^{o}C, J~ σ E
vi. Suppressed degradation rates with the polymer barriers at the grain boundary[31,32]

These extremely interesting properties can offer many new dielectrics design opportunities, along with many scientific details on the natures of the ferroelectric behavior, and conduction behavior under highly localized electric field distributions.

6.0 Electrochemical Composite Design

Solid-state battery electrodes present a unique example composite material processing which can be addressed by cold sintering. The high mobility of the active ions (e.g. Li^+ and Na^+) within the host structure is necessary for electrochemical performance but also leads to decomposition and chemical reactions between adjacent composite materials during any high temperature sintering process. To address this, we apply cold sintering to a triphasic sodium-based solid-state battery electrode system containing an active material ($Na_3V_2(PO_4)_3$), a solid electrolyte ($Na_3Zr_2Si_2PO_{12}$), and an electron-conducting carbon additive (carbon nanofiber).[33] By varying the volume fractions of these components in a cold sintered pellet, we demonstrate the modification of the partial ionic and electronic conductivities in a way that allows for the optimization of mixed conduction of the bulk which serves as the matrix for the electrochemical redox reaction of the active material.

6.1 Mixed Ionic-Electronic Composite Cathodes

In all-solid-state batteries, the liquid electrolyte is replaced with a solid electrolyte which often requires a sintering process to transform the powder into an ionically conductive polycrystalline bulk. Typically, the conventional solid-state sintering process relies on solid-state diffusion, which requires temperatures near T_m to proceed quickly; often T_{sinter} is greater than 1000°C for the best ceramic electrolytes. Temperatures greater than 600°C are known to cause extensive degradative reactions of/between the solid electrolyte, the active material, and any carbon-based additives. Thus, the elevated temperature of conventional solid-state sintering process cannot be used to easily produce triphasic composites which resemble the incumbent porous electrodes containing the active material, liquid electrolyte, and carbon. Therefore, the development of solid-state batteries would benefit from the ability to fabricate dense electrodes containing arbitrary combinations of active materials, electron-conducting phases, and ion-conducting phases without inducing the decomposition/chemical reaction of these materials during fabrication. This was the challenge that we addressed with a cold sintering approach.

A three-part investigation was conducted which demonstrated the application of cold sintering to a tunable, mixed conducting, all-solid-state cathode system based on NASICON-ceramics ($Na_3V_2(PO_4)_3$-NVP, $Na_3Zr_2Si_2PO_{12}$-NZSP) and carbon nanofiber.

First, it was confirmed that the same cold sintering parameters (375°C, 3 hours, 360 MPa, 10 wt.% NaOH) used to densify NZSP in a previous study were similarly effective in fabricating dense pellets of pure NVP. The cold sintered NVP achieves a relative density of 89±2% and a room temperature conductivity of 3.98×10^{-8} S-cm^{-1}, which is consistent with prior work. A secondary phase, Na_{4+x} (Me)P_2O_9 is unavoidably formed during cold sintering and observed in X-ray diffraction.[36]

Second, diphasic composites of NVP|NZSP and NVP|CNF were cold sintered. These composites achieve a similarly high density and are mostly phase pure, except for the NVOPO secondary phase. The generation of secondary phases at such low processing temperatures emphasizes the inevitable challenge on the horizon for co-processing of solid-state batteries by any means. The total conductivity of the biphasic composites is improved relative to the pure cold sintered NVP material; a 40NVP|60NZSP composite attains a room temperature conductivity of 5.81×10^{-6}

S.cm^{-1} while a 95NVP|5CNF composite attains a room temperature conductivity of 1.31×10^{-5} S.cm^{-1} These diphasic composites demonstrate tunable transference numbers (from 0.116 to 0.995, as measured by DC polarization) which are a solely a function of fraction of conductive additive added to the NVP active material. These results are summarized in **Figure 14**. This is the first demonstration of tunable transference numbers in an all-solid-state battery electrode, made by the low processing temperature afforded by cold sintering.

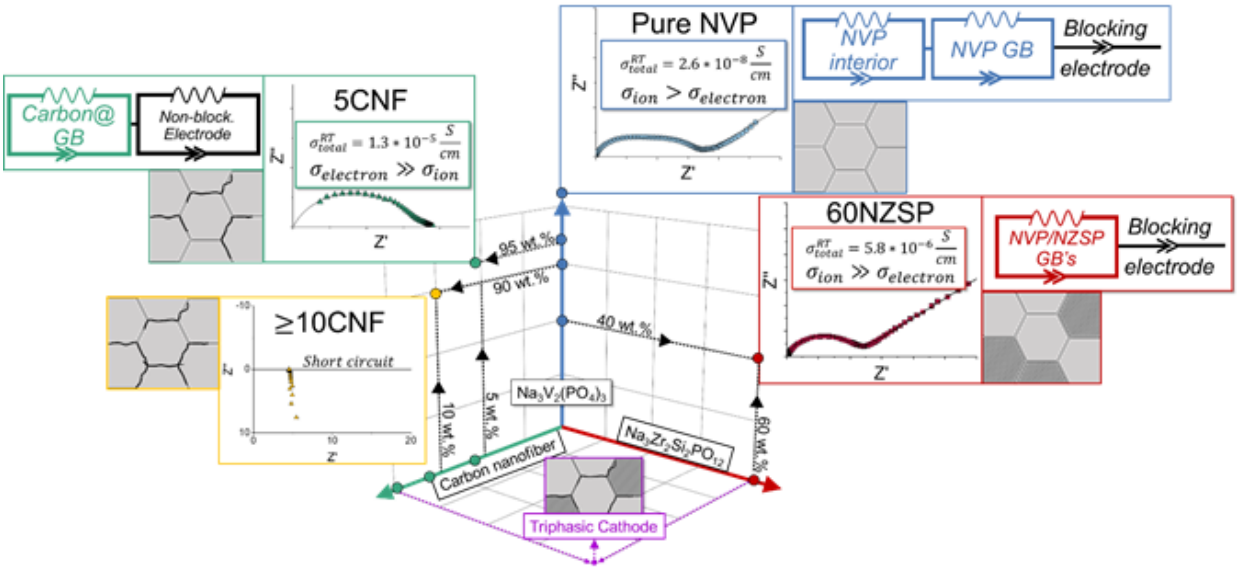

Figure 14: *The three-dimensional design space of cold sintered triphasic composites is presented schematically. Each axis represents one of the composite constituents of interest in this work (NVP, NZSP, or CNF). Points in each 2D plane therefore represent the biphasic composites presented in this study, with representative impedance responses, equivalent circuits, and idealized microstructures. The approximate composition of the triphasic composite cathode containing all three materials is also shown in the 3D space.*[37]

Cathode composites of 25|60|15 NVP|NZSP|CNF (wt.%) were cold sintered, and the intimate mixing of the respective components is obtained at a granular level, as shown in **Figure 15**.

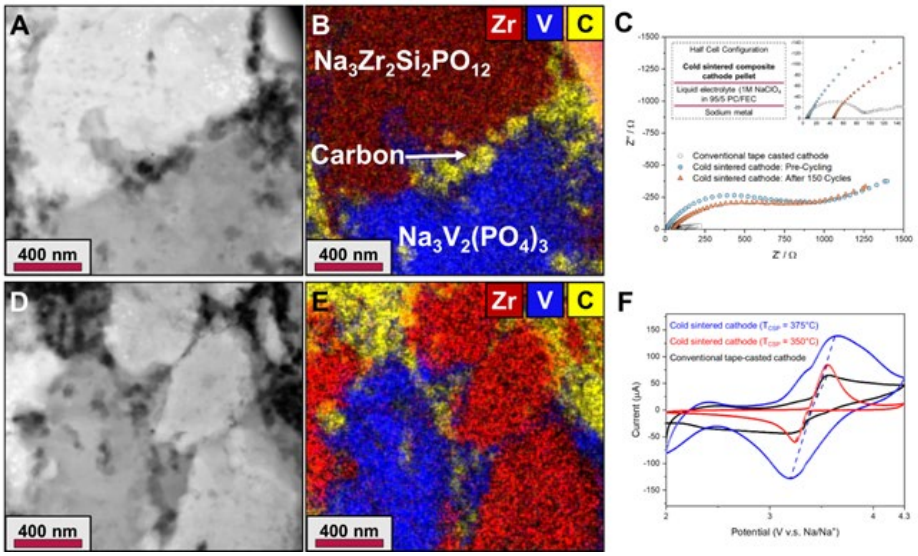

Figure 15: *STEM images of a cold sintered solid-state composite cathode are shown (**A, D**) adjacent to their respective EDS images (**B, E**). The mixed conducting microstructure is comprised of NVP active material (blue), NZSP solid electrolyte (red), and carbon nanofibers (yellow). The impedance of the cold sintered cathode half-cell compared with a conventional porous cathode half-cell is shown in (**C**). A CV plot of cold sintered cathodes (TCSP of 350°C and 375°C) compared to a conventional half-cell are shown in (**F**). The CV was conducted at room temperature with a scan rate of 0.1 mV.s^{-1}.*[37]

The thick cathodes were assembled into half-cells with liquid electrolyte and sodium metals anodes and cycled. They achieve fair capacities at room temperature (84 mAh g^{-1}), which is improved upon increased the cycling temperature to 50°C (107 mAh g^{-1}). The presence of an undesired secondary phase (NVOPO) limits the coulombic efficiency, but such effects can be minimized by reducing the cold sintering temperature. The thick cold sintered cathodes have poor rate performance, but this is consistent with similar studies of thick all-solid-state batteries.

7.0 Cermets

Cold sintering of metals may offer opportunities to develop new concepts in the design and fabrication of metallic matric composites. The concept investigated to develop cermets is based upon the (a) grain boundary engineering of metals with preceramic polymers through cold sintering, followed by the (b) heat treatment of the cold sintered metal-polymer composite at the appropriate temperature and atmosphere conditions to pyrolyze the polymer into an interfacial polymer-derived ceramic. With this approach, we could in fact expect uniform and nm-thick interfaces of silicon carbides, oxycarbides or nitrides from polycarbosilanes,

polysiloxanes or polysilazanes, respectively. This could lead to cermets with improved intergranular corrosion resistance, and tuned thermal, electrical, mechanical properties.

A preliminary test was conducted on a Fe-polydimethylsiloxane (PDMS) system. Fe powder was prepared with 1 wt.% of H_3PO_4 to form a phosphate layer facilitating cold sintering. The amorphous nature of the phosphate layer is confirmed by absence of diffraction peaks characteristic of crystalline iron phosphate (inset - **Figure 11 (**a)) and previous TEM analyses. The powder is then mixed with 5 vol.% PDMS and cold sintered at 140 °C, 700 MPa for 10 min. In the Fe-PDMS composite, the phosphate layer coating Fe grains is obvious as shown in **Figure 11** (a-c, e). At the magnification used, interfacial polymer cannot be seen. However, it appears like polymers segregate in open pores during cold sintering **Figure 11** (d). After a heat treatment at 1300 °C for 120 min in a $95N_2/5H_2$ forming gas atmosphere, the observed microstructural changes in the composite **Figure 11** (f) underscores Fe grain growth, dispersed iron phosphate inclusions, likely resulting from the extent of the thermally induced volume diffusion. Iron phosphate inclusions are either amorphous or in small amounts in the composite as they are not detected by X-Ray diffraction (inset - **Figure 11** (f)).

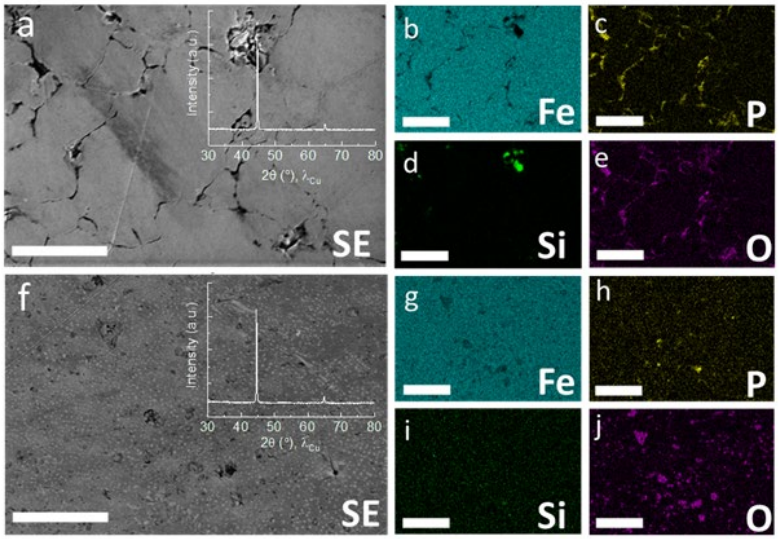

Figure 11: *EDS analysis of the Fe-PDMS composite cold sintered at 140 °C, 700 MPa and 10 min (a-e), then heat treated at 1300 °C for 120 min under 95/5 forming gas atmosphere (f-j): (a,f) secondary electron – SE – image, with XRD patterns in inset. Elemental maps of (b,g) iron – Fe, (c,h) phosphorous – P, (d,i) silicon – Si, (e,j) oxygen – O. Scale bar: 50 µm.*

8.0 Summary and Conclusions

Based on a non-equilibrium thermodynamic approach with a transient liquid, a moderate temperatures and applied pressure in an open system, we can enable a chemo-mechanical process that is enabled by a pressure solution creep process, and this can transition powder compacts into densified structures, known as cold sintering.

Cold sintering offers numerous opportunities for developing new thick film and bulk ceramics, given the low temperatures that avoid or minimizes chemical interactions with different materials permitting the design of composites and grain boundary engineering. This permits ceramics, polymers, and metals to all be densified in a single processing step and controlling interfaces from a nanometer to micrometer length scale. The low temperatures also permit metastable materials to be densified without decomposition. So cold sintering opens opportunities that were previously unavailable to materials designers.

Under this AFOSR (*FA9550-19-1-0372*) program we have classified the chemical routes that enabled the cold sintering process. We have demonstrated the composite designs in multiple materials systems with a special emphasis on functional materials that includes high energy dielectrics and electrochemical energy storage materials and mechanical applications such as metals and cermet structures.

9.0 References

1. Clive A. Randall, J.G., Hanzheng Guo, Amada Baker, Michael Lanagan, Cold sintering ceramics and composites. *US Patent 16905236 2020 (application date 2015)*
2. Baker, A., H.Z. Guo, J. Guo, and C. Randall. *Journal of the American Ceramic Society* **2016**, 99, 3202-3204.
3. Guo, J., H. Guo, A.L. Baker, M.T. Lanagan, E.R. Kupp, G.L. Messing, and C.A. Randall, Cold Sintering. *Angewandte Chemie International Edition* **2016**, 55, 11457-11461.
4. Guo, J., R. Floyd, S. Lowum, J.-P. Maria, T.H.d. Beauvoir, J.-H. Seo, and C.A. Randall,. *Annual Review of Materials Research* **2019**, 49, 275-295.
5. Kähäri, H., M. Teirikangas, J. Juuti, and H. Jantunen, *Journal of the American Ceramic Society* **2014**, 97, 3378-3379.
6. Gonzalez-Julian, J., K. Neuhaus, M. Bernemann, J. Pereira da Silva, A. Laptev, M. Bram, and O. Guillon,. *Acta Materialia* **2018**, 144, 116-128.
7. Floyd, R., S. Lowum, and J.-P. Maria,. *Review of Scientific Instruments* **2019**, 90, 055104.

8. Elissalde, C., U.C. Chung, M. Josse, G. Goglio, M.R. Suchomel, J. Majimel, A. Weibel, F. Soubie, A. Flaureau, A. Fregeac, and C. Estournès, *Scripta Materialia* **2019**, 168, 134-138.

9. Shen, H.-Z., N. Guo, L. Zhao, and P. Shen,. *Scripta Materialia* **2020**, 177, 141-145.

10. Boston, R., P.Y. Foeller, D.C. Sinclair, and I.M. Reaney,. *Inorganic Chemistry* **2017**, 56, 542-547.

11. Guo, J., S.S. Berbano, H. Guo, A.L. Baker, M.T. Lanagan, and C.A. Randall,. *Advanced Functional Materials* **2016**, 26, 7115-7121.

12. Guo, H.Z., A. Baker, J. Guo, and C.A. Randall, Cold Sintering Process. *Journal of the American Ceramic Society* **2016**, 99, 3489-3507.

13. Toda,K. Kim,S.W. Hasegawa,T., Watanabe,M., Kaneko,T., Toda,A,. R. Yamanashi, S. Kumagai, M. Muto, A. Itadani, M. Sato, K. Uematsu, T. Ishigaki, J. Koide, M. Toda, E. Kawakami, Y. Kudo, T. Masaki, D.H. Yoon, Key Eng. Mater. 751 (2017) 353–357, https://doi.org/10.4028/www.scientific.net/KEM.751.353.

14. Toda,K., Kaneko, T. Hasegawa, M. Watanabe, Y. Abe, T. Kuroi, M. Sato, K. Uematsu, S.W. Kim, Y. Kudo, T. Masaki, D.H. Yoon, Key Eng. Mater. 777 (**2018**) 163–167, https://doi.org/10.4028/www.scientific.net/KEM.777.163.

15. Kozawa,T., K. Yanagisawa, K., Suzuki, Y, J. Ceram. Soc. Japan 121 (**2013**) 308–312.

16. Watanabe, M., Inoi,J, Kim,S.W, Kaneko,T, Toda,M, Sato,M, Uematsu, K. Toda, J. Koide, M. Toda, E. Kawakami, J. Ceram. Soc. Japan 125 (**2017**) 472–475.

17. Antonova, M.M. Sov. Powder Metall, Met. Ceram 4 (**1965**) 538–544, https://doi.org/10.1007/BF00774255.

18. Funahashi,S. Kobayashi,E, Shiratsuyu, K,. Randall, J. Cer. Ass. Jap 127 (**2019**) 899.

19. Q. Li, S. Gupta, L. Tang, S. Quinn, V. Atakan, R.E. Riman, Front. Energy Res. 3 (**2016**) 1 https://doi.org/10.3389/fenrg.2015.00053.

20. Ndayishimiye,A, Sengul, MY, Sada,T Dursun,S Bang, SH, Grady, Z.A et al. Open Ceramics 2, 100019, (**2020**).

21. Urai, J.L, Spiers, C.J, Zwart, H.J, Lister. G.S. Nature 324, 554-557, (**1986**).

22. Ndayishimiye, A, Sengul,M.Y., Akbarian,D., Fan, Z., Tsuji,K., Bang, S.H, van Duin, A.C.T, Randall, C.A., Nano Letters 21 [8] (**2021**) 3451–3457.

23. Funhashi, S., Guo,J, Guo, H, Wang, K, Baker, A.L, Shiratsuya, K, and Randall, C.A, J.Am. Ceram. Soc 100, 2, 546-553 (**2017**).

24. Tsuji,K., Ndayishimiye,A,. Lowum,S., Floyd,R., Wang, K., Wetherington, M., Maria, J.P., Randall, C.A., J. Euro Cer. Soc, 40, 4, **2020**, 1280-1284.

25. Sada,T., Fan,Z., Ndayishimiye,A. Tsuji,K,. Bang, S.H., Fujioka,Y., Randall, C.A., , J. Am. Ceramic Society 104 [1] (**2021**) 96-104.

26. Zhang X., and Spiers, C.J. Geochem. Cosmochim, Acta. 69, 5681-5691, (**1986**)

27. Ndayishimiye,A., Fan,Z., Mena-Garcia,J., Anderson, J.M., Randall, C.A. Open Ceramics,11,100293, (**2022**).

28. Paradis,L, Waryoba, R Kyle, A Ndayishimiye, Z Fan, R Rajagopalan, Randall, C.A Advanced Engineering Materials 2200714, 1-11, (**2022**)

29. Liu, J., German, R.M. *Metall Mater Trans A* **30**, 3211–3217 (**1999**).

30. Sada,T., Ndayishimiye,A., Fan, Z., Fujioka,Y,. Randall, C.A, J. of Appl. Phys. 129, (**2021**) 184102.

31. Sada,T., Tsuji,K., Ndayishimiye,A., Fan,Z. Fujioka,Y., Randall, CA., Adv. Mats Interfaces, 8 (18), 2100963, (**2021**).

32. Sada,T., Tsuji,K., Ndayishimiye,A., Fan,Z. Fujioka,Y., Randall, CA., J. Appl. Phys 128, (**2020**) 084103.

33. Zhang, X. Rui, X, Chen,D., Tan,H, Yang,D., Huang, S., and Yu,Y. Nanoscale, **2019**, 11, 2556 -2576.

34. Bielefeld,A.,Weber, D.A and Janek, J. J. Phys. Chem. C, **2019**, 123, 1626–1634.

35. Miara,L., Windmüller,A,. Tsai,C.L, Richards, W.D., Ma, Q., Uhlenbruck,S, Guillon, O., Ceder,G., ACS Appl. Mater. Interfaces, **2016**, 8, 26842–26850.

36. Kovrugin,V.M., David, N. Recham, N and Masquelier, C., Inorg. Chem, **2018**, 57, 9.

37. Grady, Z.A Seo,J.H Tsuji,K., Ndayishimiye,A., Lowum, S. Dursun,S., Maria,J.P and Randall, C.A., The Electrochemical Society Interface 29 [4] (**2020**) 59-65.

38. Nie,Z. Ong,S. Hussey,D.S Lamanna,J.M., Jacobson, D.L., and. Koenig, G.M., Mol. Syst. Des.Eng., 2020, 5, 245–256.

10.0 Other Activities under this Program

10.1 Outreach: Arnaud Ndayishimiye

- Invited Panelist: African Innovation, Fourth Annual Conference / Pan-African Professional Alliance (State College, virtual conference, April 2021)

10.2 Talks: Clive Randall

- Plenary lecture, AMF-AMEC 2021 (Thailand; virtual meeting, July 2021)
- Invited Talk 125th College of Earth and Mineral Sciences, The Pennsylvania State University, Virtual Seminar (June 2021)
- Invited lecture, IEEE-ISAF-PFM 2021 (Australia; virtual meeting, May 2021)
- Invited lecture, European Ceramic Society Electroceramics XVII Conference – Darmstadt, Germany (virtual meeting – 2020)
- Invited Lecture, Sustainability in Functional Materials Research NTNU (Norway, Virtual Meeting, May 2021)
- Keynote International Electronics Conference on Actuators, (Portugal, Virtual Meeting)
- Dept Material Science and Engineering, Rutgers, Virtual seminar Dec 2020.
- Dept Material Science and Engineering, RPI, Virtual Seminar Feb 2021.
- Invited: International Symposium for Application of Ferroelectrics, Tours France, (27 June – July 1, 2022)
- Invited Talk: European Ceramic Society, Krakow, Poland, (10-14 July,2022)
- Invited Teacher: European Ceramic Society: Sintering, Krakow, Poland, (8-10, July 2022)
- Virtual Invited Talk: Power Electronics and Energy Conversion Workshop, (Hosted Sandia National Labs) (24th August 2022)
- Invited US-Japan Workshop on Dielectrics and Piezoelectrics- Charlotte South Carolina, USA, Nov 13-19, (2022).
- Plenary Lecturer: German Ceramics Society- Jena Germany, 28 March (2023)
- P.I Ceramics: Germany (23 March 2023)
- Invited Scientific Colloquium on Material Science, Arlberg, Austria, (April 18, 2023)
- Materials Science Dept. Leoban, Austria, (April 21, 2023)
- Material Science Dept. Queen Mary College, London, UK (May 6, 2023)
- College of Science, University of East Anglia, Norwich, UK (May 9, 2023)
- Knowles Electronic Components, Norwich, (May 10, 2023)
- Taiyo Yuden, Japan, (May 22, 2023)
- Invited Talk: Ferroelectrics Meeting of Asia (FMA), Kyoto Japan, (May 26, 2023)
- Kyocera R&D Headquarters, Kagashima, Japan, (May 28, 2023)
- Murata R&D Laboratories, Kyoto, Japan, (May 30, 2023),
- College of Engineering Sciences, Osaka Metropolitan University, (May 31, 2023)
- 2 -Invited Talks at European Ceramic Society Meeting, Lyon, France, (4 and 5 July 2023)

10.3 Talks: Zane Grady

- EMA 2021, January 2021. Cold sintering solid electrolytes and electrode composites for solid-state sodium ion batteries, Authors: Zane Grady, Arnaud Ndayishimiye, Zhongming Fan, Clive Randall
- ECERS, July 2020 "Cold sintering of sodium ion cathodes and electrolytes for all solid-state batteries" Authors: Zane Grady, Arnaud Ndayishimiye, Joo Hwan-Seo, Clive Randall

10.4 Talks: Arnaud Ndayishimiye

- Oxide seminar, April 2020. Cold Sintering: Status and prospects, Authors: Arnaud Ndayishimiye, Clive Randall, CSP Team (The Pennsylvania State University, Virtual meeting)

10.5 Dissertations

Zane Grady, Ph.D Dissertation, "Cold Sintering of Solid State Sodium Ion Battery Components," The Pennsylvania State University, **(May 2023).**

10.6 Awards:

IEEE Distinguished Lecturer (2019-2020)

Distinguished Professor of Material Science and Engineering (2020)

American Ceramics Society Orton Lecture (2021)

National Academy of Inventors (2022)

College Faculty Student Mentoring Award (2023)

10.7 Student Award

Zane Grady

Robert Newham Annual Award For Crystal Chemistry, Material Science and Engineering Dept Award for Graduate Students.